

MODELING THE LID DRIVEN FLOW: THEORY AND COMPUTATION

MAKRAM HAMOUDA^{1,2}, ROGER TEMAM² AND LE ZHANG²

Abstract. Motivated by the study of the corner singularities in the so-called cavity flow, we establish in the first part of this article, the existence and uniqueness of solutions in $L^2(\Omega)^2$ for the Stokes problem in a domain Ω , when Ω is a smooth domain or a convex polygon. This result is based on a new trace theorem and we show that the trace of u can be arbitrary in $L^2(\partial\Omega)^2$ except for a standard compatibility condition recalled below. The results are also extended to the linear evolution Stokes problem. Then in the second part, using a finite element discretization, we present some numerical simulations of the Stokes equations in a square modeling thus the well known lid-driven flow. The numerical solution of the lid driven cavity flow is facilitated by a regularization of the boundary data, as in other related equations with corner singularities ([9], [10], [45], [24]). The regularization of the boundary data is justified by the trace theorem in the first part.

Key words. Stokes and related (Oseen, etc.) flows, weak solutions, existence, uniqueness, regularity theory, lid driven cavity.

Introduction

We are interested in the first part of this article in the existence of L^2 -solutions for the (linear stationary) Stokes problem in a domain Ω of \mathbb{R}^2 . The set Ω is assumed to be bounded, regular of class \mathcal{C}^2 , or it could be a convex polygonal domain. More generally Ω can be what we will call a (convex) *domain of polygonal type* that is Ω a piecewise \mathcal{C}^2 domain for which the tangent to the boundary Γ has a finite number of discontinuity points S_1, \dots, S_N , with a well defined left and right tangent at these points, the angle between the tangents being $0 < \alpha_j < \pi$; hence the domain Ω needs not be convex in this case, we only require the angles to be convex.

Motivated by the study of a flow in such a domain Ω (see Part 2) we start with the stationary linear Stokes problem, which, in its most general form reads:

$$(1) \quad \begin{cases} -\Delta \tilde{u} + \nabla \tilde{p} = f & \text{in } \Omega, \\ \operatorname{div} \tilde{u} = h & \text{in } \Omega, \\ \tilde{u} = g & \text{on } \Gamma = \partial\Omega. \end{cases}$$

The emphasis in the second part of this article is on the so-called lid-driven cavity problem. In this case Ω is the square $(0, 1) \times (0, 1)$, $f = h = 0$ and $g = (0, 0)$ at $x = 0, 1$, and $y = 0$, and $g = (1, 0)$, at $y = 1$; the discontinuities of g produce singularities and vortices at the corners $(0, 1)$ and $(1, 1)$. We describe this example in more detail in Section 3 and in Part 2 where we exhibit some numerical simulations related to the lid-driven cavity problem using the classical finite element discretization method together with a regularization of the boundary values of the velocity justified by the results in Part 1.

We know that if $f \in L^2(\Omega)^2$, $h = g = 0$, then the existence and uniqueness of a solution $\tilde{u} \in H_0^1(\Omega)^2$ of (1) is derived from the projection theorem, and $\tilde{p} \in L^2(\Omega)$

follows from the result of Deny-Lions [13]; see also [59], [60]. If $f \in L^2(\Omega)^2$ and $h \in L^2(\Omega)$, with $\int_{\Omega} h dx dy = 0$, we have existence and uniqueness of $U \in H^2(\Omega)^2, P \in H^1(\Omega)$ satisfying

$$(2) \quad \begin{cases} -\Delta U + \nabla P = f & \text{in } \Omega, \\ \operatorname{div} U = h & \text{in } \Omega, \\ U = 0 & \text{on } \Gamma. \end{cases}$$

In the case where Ω is smooth, this result is proved in [8]; see also [31]. When Ω is of polygonal type, this result is proven in [32]; see also [33]. The difference $u = \tilde{u} - U, p = \tilde{p} - P$ is solution of the following problem which concentrates the lack of regularity on the boundary value, like for the lid driven cavity problem:

$$(3) \quad \begin{cases} -\Delta u + \nabla p = 0 & \text{in } \Omega, \\ \operatorname{div} u = 0 & \text{in } \Omega, \\ u = g & \text{on } \Gamma. \end{cases}$$

In Section 1 we derive a trace theorem for functions u in $L^2(\Omega)^2$ satisfying (3)₁, (3)₂, thus giving a meaning to (3)₃. Then in Section 2 we establish the existence and uniqueness of a solution $u \in L^2(\Omega)^2$ of (3) provided $\int_{\Gamma} g \cdot n \, d\Gamma = 0$, see Theorem 3; here n is the unit outward normal vector on Γ and below τ is the unit tangent vector, such that n is directly orthogonal to τ . We discuss in more details an example of lid driven cavity flow in Section 3. Finally in Section 4 we extend the results to the linear evolution Stokes problem. Namely, we prove the necessary trace theorems, then, in Theorem 5, we show that if g is given in $L^2(0, T; L^2(\Gamma)^2)$ satisfying $\int_{\Gamma} g \cdot n \, d\Gamma = 0$ for a.e. $t \in (0, T)$, then there exists a unique solution $u \in L^2(0, T; L^2(\Omega)^2)$ of

$$(4) \quad \begin{cases} \frac{\partial u}{\partial t} - \Delta u + \nabla p = 0 & \text{in } (0, T) \times \Omega, \\ \operatorname{div} u = 0 & \text{in } \Omega, \\ u = g & \text{on } (0, T) \times \Gamma, \\ u(0) = 0, \end{cases}$$

with $p \in \mathcal{D}'((0, T) \times \Omega)$.

There is a large literature on weak solutions of the Navier-Stokes equations starting with the now classical results of J. Serrin [53] of solutions of the Navier-Stokes equations in $L^r(0, T; L^s)$ up to the recent result [27] of uniqueness of solutions in $L^3(0, T; L^3(\mathbb{R}^3)^3)$, itself followed by a series of articles improving and simplifying its proof.

In another direction Fabes, Kenig and Verchota study in [18] the stationary Stokes problem on Lipschitz domains of $\mathbb{R}^n, n \geq 3$, using methods of harmonic analysis. This work is extended to the time-dependent case in the articles [52], [51] which study the evolution Stokes equation in a Lipschitz domain of $\mathbb{R}^n, n \geq 3$, in L^2 space in [52] and in some L^p spaces in [51].

In yet another direction, H. Amann introduced in [2] and [1] a concept of weak solutions for the Navier-Stokes equations using the concept of duality or adjoint equations. The idea is to integrate by parts all or most of the derivatives against a smooth test function. The whole book [41] is devoted to constructing such weak solutions of linear elliptic and parabolic equations, but they do not address the case of the Stokes equations. The work of [1, 2] has been subsequently extended in different directions (Stokes vs Navier-Stokes, stationary vs time dependent, space L^2 vs spaces L^p) in a series of articles [22], [21], [23], [20]; see also [46], [43]. These

articles are mostly concerned with space dimension $n = 3$, and smooth domains, However as explained in [22, b], one of the difficulties is to give a meaning to the trace of u and to verify the boundary condition $u = g$ on Γ . Either this question is ignored or some partial results are established. The object of this article is to establish a clear trace theorem and to give a precise sense to the boundary condition $u = g$ on Γ when $u \in L^2(\Omega)^2$ satisfies (3)₁ and (3)₂. A result related to ours appear in [3], but it is limited to the time independent case.

We conclude this introduction with an a priori estimate borrowed from [36] which we reproduce for the sake of completeness.

Lemma 1. *Assume that u, p and g are sufficiently regular (e.g. $u \in H^2(\Omega)^2, p \in H^1(\Omega), g \in H^{3/2}(\Gamma)^2$) and satisfy (3). Then*

$$(5) \quad |u|_{L^2(\Omega)^2} \leq c_1 |g|_{L^2(\Gamma)^2},$$

where the constant c_1 depends only on Ω .

Proof. The proof is based on a transposition argument used for general elliptic problems by Lions and Magenes [41].

We consider v, q solution of the adjoint problem

$$(6) \quad \begin{cases} -\Delta v + \nabla q = u & \text{in } \Omega, \\ \operatorname{div} v = 0 & \text{in } \Omega, \\ v = 0 & \text{on } \Gamma. \end{cases}$$

We know from the references quoted above that, at least, $v \in H^2(\Omega)^2, q \in H^1(\Omega)$ so that the following integrations by parts make sense. We have, n denoting the outside unit normal on Γ :

$$\begin{aligned} \int_{\Omega} |u|^2 d\Omega &= \int_{\Omega} u \cdot (-\Delta v + \nabla q) \, d\Omega, \\ &= (\text{since } v = 0 \text{ on } \Gamma \text{ and } \operatorname{div} u = \operatorname{div} v = 0) \\ &= - \int_{\Gamma} g \cdot \frac{\partial v}{\partial n} \, d\Gamma - \int_{\Omega} \Delta u \cdot v \, d\Omega + \int_{\Gamma} g \cdot n q \, d\Gamma \\ &= - \int_{\Gamma} (g \cdot \frac{\partial v}{\partial n} - g \cdot n \cdot q) \, d\Gamma \\ &\leq |g|_{H^{-1/2}(\Gamma)^2} | \frac{\partial v}{\partial n} |_{H^{1/2}(\Gamma)^2} + |g \cdot n|_{H^{-1/2}(\Gamma)} |q|_{H^{1/2}(\Gamma)} \\ &\leq c |g|_{H^{-1/2}(\Gamma)^2} (|v|_{H^2(\Omega)^2} + |q|_{H^1(\Omega)}) \\ &\leq (\text{using the } H^2(\Omega) \text{ regularity for (6)}) \\ &\leq c |g|_{H^{-1/2}(\Gamma)^2} |u|_{L^2(\Omega)} \\ &\leq c |g|_{L^2(\Gamma)^2} |u|_{L^2(\Omega)}. \end{aligned}$$

The lemma is proven.

Remark 1. It follows from the proof of Lemma 1 that we can replace $|g|_{L^2(\Gamma)^2}$ by $|g|_{H^{-1/2}(\Gamma)^2}$ in the right-hand side of (5). We will not use this improvement here because it is not easy to compute $|g|_{H^{-1/2}(\Gamma)^2}$.

Remark 2. In the above we have used the $H^2 - H^1$ regularity for the Stokes problem, that is $v \in H^2(\Omega)^2, q \in H^1(\Omega)$ when $u \in L^2(\Omega)^2$. This is classical when Ω is smooth, say C^2 (see e.g. [8], [31]), and is proven in [33], [32] for the type of polygonal domains we are considering.

Part 1. A trace theorem and application

We study in this part the existence issue of the Stokes equations when the domain has some corners, namely here the square, but our results extend to any domain with convex corners with some additional technicalities that have to be taken into account. One of the major issues for this problem is to define the trace of the very weak Stokes solutions at the singular part of the boundary. This will be the objective of this part both for the stationary and the time-dependent Stokes problems.

1. A trace theorem

We want to define the trace on Γ of a function $u \in L^2(\Omega)^2$ which satisfies (3)_{1,2} for some distribution $p \in \mathcal{D}'(\Omega)$. We first recall (see e.g. [59, Theorem 1.2, Chap. 1]), that if $u \in L^2(\Omega)^2$ and $\operatorname{div} u \in L^2(\Omega)$, the trace of its normal component $\gamma_n(u) = u_n|_\Gamma$ is defined and belongs to $H^{-1/2}(\Gamma)$. Hence we only need to define the trace of its tangential component $\gamma_\tau(u) = u \cdot \tau|_\Gamma$.

We will make use of the following result from Héron [37].

Theorem 1. Let

$$Y_2(\Omega) = \{v \in H^2(\Omega)^2, \operatorname{div} v = 0\}.$$

Then a pair $(g_0, g_1) \in H^{3/2}(\Gamma)^2 \times H^{1/2}(\Gamma)^2$ is the trace on Γ of $(\gamma_0(v), \gamma_1(v)) = (v, \frac{\partial v}{\partial n})$, where $v \in Y_2(\Omega)$, if and only if

$$(7) \quad \int_{\Gamma} g_0 \cdot n \, d\Gamma = 0,$$

and

$$(8) \quad \operatorname{div}_{\Gamma} (g_0)_\tau + g_1 \cdot n - 2K \, g_0 \cdot n = 0,$$

where $\operatorname{div}_{\Gamma}$ is the tangential divergence on Γ , $(g_0)_\tau$ the tangential component of g_0 and K is the algebraic curvature of Γ .

When we restrict to $g_0 = 0$, we obtain the following Corollary.

Corollary 1. Let

$$X_2(\Omega) = \{v \in H^2(\Omega), \operatorname{div} v = 0, v = 0 \text{ on } \Gamma\}.$$

Then $g_1 \in H^{1/2}(\Gamma)^2$ is the trace $\gamma_1(v)$ of $\partial v / \partial n$ on Γ where $v \in X_2(\Omega)$, if and only if

$$(9) \quad g_1 \cdot n = 0 \quad \text{on } \Gamma,$$

or alternatively if and only if

$$(10) \quad g_1 \in H_{\tau}^{1/2}(\Gamma)^2,$$

the space of tangential vectors in $H^{1/2}(\Gamma)^2$.

Furthermore γ_1 is surjective and continuous from $X_2(\Omega)$ onto $H_{\tau}^{1/2}(\Gamma)^2$, and it possesses a continuous left inverse R (lifting operator), that is $R\gamma_1 = I$.

Proof. The condition (9) - (10) is just the restriction of (7) - (8) to the case $g_0 = 0$. Of course the trace operator is continuous and since it is surjective, it is also continuous and one to one from the orthogonal of its kernel in $X_2(\Omega)$, $(\operatorname{Ker} \gamma_1)^{\perp}$ onto $H_{\tau}^{1/2}(\Gamma)^2$. By the closed graph theorem it is bicontinuous from $(\operatorname{Ker} \gamma_1)^{\perp}$ to $H_{\tau}^{1/2}(\Gamma)$ and its inverse R is a left inverse of γ_1 . The proof is complete.

Remark 3. In [37] Theorem 1 is proved by assuming that Γ is \mathcal{C}^3 ; the role of the regularity of Γ is explained p. 1303. Theorem 1 extends to domains of polygonal type.

We now want to define the tangential trace on $\Gamma, \gamma_\tau(u)$, for a function u which satisfies

$$(11) \quad \begin{cases} \Delta u = \nabla p & \text{in } \Omega, \\ \operatorname{div} u = 0 & \text{in } \Omega, \end{cases}$$

for some distribution $p \in \mathcal{D}'(\Omega)$. Note that, by De Rham's theory (see e.g. Deny and Lions [13, Theorem 1.1]), the set

$$F(\Omega) := \{u \in L^2(\Omega)^2 \text{ satisfying (11)}\},$$

is closed in $L^2(\Omega)^2$, and is hence a Hilbert space for the norm of $L^2(\Omega)^2$. Note also that since $u \in L^2(\Omega)^2, \Delta u \in H^{-2}(\Omega)^2$ and by the results of Deny and Lions [13] and the analogue of Proposition 1.2 in [59], $p \in H^{-1}(\Omega)$.

The construction of $\gamma_\tau(u)$ will somehow mimic the construction of $\gamma_n(u) = u \cdot n|_\Gamma$ in [59].

Theorem 2. *Assume that Γ is of class \mathcal{C}^2 or is of polygonal type. Then there exists a linear continuous operator $\gamma_\tau \in \mathcal{L}(F(\Omega), H_\tau^{-1/2}(\Gamma)^2)$, such that*

$$(12) \quad \gamma_\tau u = u \cdot \tau|_\Gamma \text{ for every } u \in F(\Omega) \cap \mathcal{C}^2(\bar{\Omega})^2.$$

The following generalized Stokes formula is valid for all $u \in F(\Omega)$ and $g_1 \in H_\tau^{1/2}(\Gamma)^2$:

$$(13) \quad \langle \gamma_\tau u, g_1 \rangle = \int_\Omega u \cdot \Delta v \, d\Omega,$$

where v is any function of $X_2(\Omega)$ such that $\gamma_1(v) = g_1$.

Proof. For $u \in F(\Omega)$ and $g_1 \in H_\tau^{1/2}(\Gamma)^2$, we consider the expression

$$(14) \quad L_u(g_1) = \int_\Omega u \cdot \Delta v \, d\Omega,$$

where v is any function in $X_2(\Omega)$ such that $\gamma_1(v) = g_1$. For the coherence of the definition we first need to show that the expression (14) is independent of the choice of v . If v_1, v_2 are two such choices, and $v = v_1 - v_2$, we must show that

$$(15) \quad \int_\Omega u \cdot \Delta v \, d\Omega = 0,$$

whenever $v \in X_2(\Omega)$ and $\gamma_1(v) = 0$. In this case

$$(16) \quad v \in \tilde{X}_2(\Omega) = \{v \in H_0^2(\Omega), \operatorname{div} v = 0\}.$$

We prove below, in Lemma 2 that

$$(17) \quad \mathcal{V} = \{v \in \mathcal{D}(\Omega)^2, \operatorname{div} v = 0\}$$

is dense in $\tilde{X}_2(\Omega)$. Then to prove (15) we observe that, for $v \in \mathcal{V}$,

$$\begin{aligned} \int_\Omega u \cdot \Delta v \, d\Omega &= \langle u, \Delta v \rangle_{\mathcal{D}, \mathcal{D}'} \\ &= \langle \Delta u, v \rangle_{\mathcal{D}, \mathcal{D}'} = - \langle p, \operatorname{div} v \rangle_{\mathcal{D}, \mathcal{D}'}, \end{aligned}$$

and this expression vanishes since $v \in \mathcal{V}$.

In addition, if we write (14) with $v = Rg_1$, R the left-inverse of γ_1 given by Corollary 1, we observe that the expression $L_u(g_1)$ is linear continuous on $H_\tau^{1/2}(\Gamma)^2$ as indeed

$$\begin{aligned} |L_u(g_1)| &= \left| \int_{\Omega} u \Delta(Rg_1) \, d\Omega \right| \\ &\leq |u|_{L^2(\Omega)^2} |\Delta(Rg_1)|_{L^2(\Omega)^2} \\ &\leq c |u|_{L^2(\Omega)^2} |Rg_1|_{H^2(\Omega)^2} \\ &\leq c |g_1|_{H_\tau^{1/2}(\Gamma)^2}. \end{aligned}$$

Finally, to prove (12) we observe that if $u \in F(\Omega) \cap C^2(\bar{\Omega})^2$ and $v \in X_2(\Omega)$ then the following integrations by parts are legitimate:

$$\begin{aligned} \int_{\Omega} u \Delta v \, d\Omega &= \int_{\Omega} \Delta u \, v + \int_{\Gamma} \left(u \frac{\partial v}{\partial n} - \frac{\partial u}{\partial n} v \right) d\Gamma \\ &= \int_{\Gamma} u \frac{\partial v}{\partial n} d\Gamma + \int_{\Omega} \nabla p \, v \, d\Omega \\ &= \int_{\Gamma} u \frac{\partial v}{\partial n} \, d\Gamma + \int_{\Gamma} p \, v \, n \, d\Gamma - \int_{\Omega} p \operatorname{div} v \, d\Omega \\ &= \int_{\Gamma} u \frac{\partial v}{\partial n} \, d\Gamma = 0. \end{aligned}$$

We are left with proving the following:

Lemma 2. \mathcal{V} is dense in $\tilde{X}_2(\Omega)$.

Proof. It is clear that $\mathcal{V} \subset \tilde{X}_2(\Omega)$. We will prove the lemma by showing that any linear continuous form ℓ on $\tilde{X}_2(\Omega)$ which vanishes on \mathcal{V} is equal to zero.

We observe that $\tilde{X}_2(\Omega)$ is a closed subspace of $(H^2(\Omega) \cap H_0^1(\Omega))^2$ and, noticing that $|\Delta v|_{L^2(\Omega)}$ is a norm on $H^2(\Omega) \cap H_0^1(\Omega)$, we see that ℓ is necessarily of the form

$$\ell(v) = \int_{\Omega} \phi \Delta v \, d\Omega,$$

for some $\phi \in L^2(\Omega)^2$. We now write that ℓ vanishes on \mathcal{V} :

$$\begin{aligned} 0 = \ell(v) &= \int_{\Omega} \phi \Delta v \, d\Omega = \langle \phi, \Delta v \rangle_{\mathcal{D}, \mathcal{D}'}, \\ &= \langle \Delta \phi, v \rangle_{\mathcal{D}, \mathcal{D}'}, \quad \forall v \in \mathcal{V}. \end{aligned}$$

But this classically implies that $\Delta \phi = \nabla \pi$ for some $\pi \in \mathcal{D}'(\Omega)$ which actually belongs to $H^{-2}(\Omega)$ as observed above.

Now for any $v \in \tilde{X}_2(\Omega)$, $\nabla \pi = \Delta \phi \in H^{-2}$ and

$$\ell(v) = \langle \nabla \pi, v \rangle_{H^{-2}, H^2}.$$

This expression vanishes because $v \in H_0^2(\Omega)^2$. Indeed using the fact that $\nabla \pi \in H^{-2}(\Omega)$, we see that

$$\begin{aligned} \langle \nabla \pi, v \rangle_{H^{-2}, H_0^2} &= \lim_{j \rightarrow \infty} \langle \nabla \pi, v_j \rangle_{H^{-2}, H_0^2} = - \lim_{j \rightarrow \infty} \langle \pi, \operatorname{div} v_j \rangle_{H^{-1}, H_0^1} \\ &= - \langle \pi, \operatorname{div} v \rangle_{H^{-1}, H_0^1}, \end{aligned}$$

where $v_j \in \mathcal{D}(\Omega)^2$ converges to v in $H_0^2(\Omega)^2$ (not necessarily in $\tilde{X}_2(\Omega)$). In the end

$$\langle \nabla \pi, v \rangle_{H^{-2}, H_0^2} = \langle \pi, \operatorname{div} v \rangle = 0.$$

2. The main theorem (Time independent case)

Our aim is now to prove the existence and uniqueness of a solution $u \in L^2(\Omega)^2$ for (3) when g is given in $L^2(\Gamma)^2$.

Theorem 3. *We assume that Ω is of class C^2 or is of polygonal type, and that g is given in $L^2(\Gamma)^2$ satisfying*

$$(18) \quad \int_{\Gamma} g \cdot n \, d\Gamma = 0.$$

Then there exists a unique solution $u \in L^2(\Omega)^2$ satisfying (3) for some $p \in \mathcal{D}'(\Omega)$.

Proof. It is easy to construct a sequence $\tilde{g}_j \in H^{3/2}(\Gamma)^2$ (or possibly more regular), which converges to g in $L^2(\Gamma)^2$. Considering then

$$(19) \quad g_j = \tilde{g}_j - \frac{1}{|\Gamma|} \left(\int_{\Gamma} \tilde{g}_j \cdot n \, d\Gamma \right) n,$$

we see that the g_j belong (at least) to $H^{3/2}(\Gamma)^2$, satisfy (18) and converge to g in $L^2(\Gamma)^2$.

For each j , thanks to [8] when Ω is of class C^2 , and to [32] when Ω is of polygonal type, we infer the existence of $(u_j, p_j) \in H^2(\Omega)^2 \times H^1(\Omega)$, satisfying (3) with g replaced by g_j . We see, thanks to Lemma 1, that the sequence u_j is bounded in $L^2(\Omega)^2$. More precisely, as observed before, the sequence u_j is bounded in $F(\Omega)$. As $j \rightarrow \infty$, we infer the existence of $u \in F(\Omega)$ and a subsequence still denoted u_j such that

$$u_j \rightarrow u \text{ weakly in } F(\Omega),$$

that is weakly in $L^2(\Omega)^2$, and u satisfies

$$\begin{aligned} -\Delta u + \nabla p &= 0 \text{ in } \Omega, \\ \operatorname{div} u &= 0 \text{ in } \Omega, \end{aligned}$$

for some distribution $p \in \mathcal{D}'(\Omega)$.

In addition, the trace theorem from [59] for γ_n , and the trace Theorem 2 above for γ_τ , tell us that $\gamma_0(u_j) = g_j$ converges to $\gamma_0(u) = g$ in $H^{-1/2}(\Gamma)^2$. Hence u satisfies (3).

It remains to show the uniqueness of solution of (3). If $(u_1, p_1), (u_2, p_2)$ are two solutions of (3) and if $u = u_1 - u_2, p = p_1 - p_2$, then

$$(20) \quad \begin{cases} -\Delta u + \nabla p = 0 & \text{in } \Omega, \\ \operatorname{div} u = 0 & \text{in } \Omega, \\ \gamma_0(u) = 0 & \text{on } \Gamma. \end{cases}$$

We must show that $u = p = 0$. We consider (v, q) defined by (6) as in the proof of Lemma 1. Note that $v \in X_2(\Omega)$, and $q \in H^1(\Omega)$. We then write

$$(21) \quad \begin{aligned} \int_{\Omega} |u|^2 d\Omega &= - \int_{\Omega} u \Delta u \, d\Omega + \int_{\Omega} u \nabla q \, d\Omega \\ &= (\text{using (13) and } \gamma_0(u) = 0) \\ &= \int_{\Omega} u \nabla q \, d\Omega. \end{aligned}$$

According to the integration by parts formula I. (1.9) in [59], this last expression is equal to

$$-(\operatorname{div} u, q) + (\gamma_n(u), \gamma_0(q)),$$

and, it thus vanishes since $\gamma_n(u) = 0$ by (20)₃ and $\operatorname{div} u = 0$ by (20)₂.

We conclude that $u = 0$, thus proving the uniqueness.

Remark 4. Another way to approach the problem (3) would be to introduce the stream function Ψ such that $u = (u_1, u_2)$ and $u_1 = \partial\Psi/\partial y, u_2 = -\partial\Psi/\partial x$ and then (3) reduces to a biharmonic problem for Ψ

$$(22) \quad \begin{cases} \Delta^2\Psi = 0 \text{ in } \Omega, \\ \frac{\partial\Psi}{\partial\tau} = -g \cdot n, \quad \frac{\partial\Psi}{\partial n} = -g \cdot \tau \text{ on } \Gamma. \end{cases}$$

After integration of the second equation in (22), Ψ would be prescribed on Γ as a primitive of $-g \cdot n$. In the simpler case where $g \cdot n = 0, \Psi = 0$ on Γ and the problem is then to find a solution Ψ of (22) in $H^1(\Omega)$. When Ω is smooth such problems are treated in Lions and Magenes [41], although the problem (22) is not explicitly mentioned in [41]. When Ω is a convex polygon or a domain of *polygonal type*, the methods of [33], [32] might apply but this remains to be done.

Remark 5. Various results describing the behavior of a fluid in a domain with corners appear in [4], [14], [50]; see also the references quoted above and their bibliography. In the engineering and fluid mechanics literature see [38], [42], [48] and [49].

3. Example for a lid driven cavity flow

We are interested in the cavity flow where $\Omega = (0, 1) \times (0, 1)$ and the velocity on Γ is $(0, 0)$ at $x = 0, 1$, and $y = 0$ and, at $y = 1, g = (1, 0)$. This is a classical model problem in computational fluid dynamics which has been the object of many studies see e.g. [5], [6], [7], [16], [17], [25], [26], [29], [30], [35], [34] - in dimension 3 -, [54] and the references therein. See also [11], [12], [15]. The singularities at the corners $(0, 1), (1, 1)$ remain a substantial computational difficulty. In [61] the author addresses this difficulty by replacing g by a continuous function g_ε which converges to g in $L^2(\Gamma)^2$ as $\varepsilon \rightarrow 0$. Such an approach has been successfully applied to the Korteweg de Vries and nonlinear Schrödinger equations, to deal with incompatible data; see [24] and [45]; see also [9], [10] and see [59] regarding incompatible initial data.

We can approximate g by g_ε which is identical to g except for the first component which is equal to

$$(23) \quad 1 - \sigma(x)e^{-x/\varepsilon} - \sigma(1-x)e^{-(1-x)/\varepsilon},$$

where σ is a smooth function

$$\sigma(x) = \begin{cases} 1, & 0 \leq x \leq 1/2 \\ \in [0, 1], & \frac{1}{2} \leq x \leq \frac{3}{4} \\ 0, & \frac{3}{4} \leq x \leq 1. \end{cases}$$

Both g and g_ε satisfy the necessary conditions

$$(24) \quad \int_{\Gamma} g \cdot n \, d\Gamma = \int_{\Gamma} g_\varepsilon \cdot n \, d\Gamma = 0.$$

It is clear that g_ε converges to g in $L^2(\Gamma)^2$ as $\varepsilon \rightarrow 0$. In view of Theorem 3, there exists a unique solution (u, p) to the problem (3) with $u \in L^2(\Omega)^2$, and a (unique) solution $(u_\varepsilon, p_\varepsilon)$ to the problem (3) with g replaced by g_ε , and $u_\varepsilon \in L^2(\Omega)^2$; as usual

the uniqueness of p_1, p_ε is meant up to the addition of a constant. In addition, when $\varepsilon \rightarrow 0$,

$$(25) \quad g_\varepsilon \rightarrow g \text{ in } L^2(\Gamma)^2,$$

and consequently

$$(26) \quad u_\varepsilon \rightarrow u \text{ in } L^2(\Omega)^2.$$

Remark 6. If one wants to focus on one of the corner singularities only, one can consider the following variations of the cavity problem

- i) For the corner $(0, 1) : g^b$ is equal to g except the first component which is equal to y at $x = 1$. Then g_ε^b is the same as g^b except the first component which is equal to

$$1 - \sigma(y)e^{-y/\varepsilon},$$

on $y = 1$.

- ii) For the corners $(1, 1) : g^\sharp$ is equal to g except the first component which is equal to y at $x = 0$. Then g_ε^\sharp is the same as g^\sharp except the first component which is equal to

$$1 - \sigma(1 - y)e^{-(1-y)/\varepsilon},$$

on $y = 1$.

It is clear that the analogues of (24), (25), (26) are still valid in this case.

4. The Time dependant case

We now want to derive the analogue of Theorem 2 in the time dependent case. We consider $T > 0$ and set $Q_T = \Omega \times (0, T), \Gamma_T = \Gamma \times (0, T)$, and we are interested in very weak solutions (in $L^2(Q_T)$) of the linearized evolution Stokes problem

$$(27) \quad \begin{cases} \frac{\partial \tilde{u}}{\partial t} - \Delta \tilde{u} + \nabla \tilde{p} = f & \text{in } Q_T, \\ \operatorname{div} \tilde{u} = h & \text{in } Q_T, \\ \tilde{u} = g & \text{on } \Gamma_T, \\ \tilde{u}(0) = u_0 & \text{in } \Omega. \end{cases}$$

As in the stationary case, with results similar in two dimensions to those of [56], [57], we can introduce a lifting of f, h , and u_0 , by considering the solution U, P of

$$(28) \quad \begin{cases} \frac{\partial U}{\partial t} - \Delta U + \nabla P = f & \text{in } Q_T, \\ \operatorname{div} U = h & \text{in } Q_T, \\ U = 0 & \text{on } \Gamma_T, \\ U(0) = u_0. \end{cases}$$

The results similar to those of [56], [57], guarantee enough regularity for f, h, u_0^1 , and then $u = \tilde{u} - U, p = \tilde{p} - P$ are solutions of

$$(29) \quad \begin{cases} \frac{\partial u}{\partial t} - \Delta u + \nabla p = 0 & \text{in } Q_T, \\ \operatorname{div} u = 0 & \text{in } Q_T, \\ u = g & \text{on } \Gamma_T, \\ u(0) = 0. \end{cases}$$

¹As we said, motivated by the lid driven cavity flow, we are interested in low regularity in g but assume f, h, u_0 are as smooth as desirables.

For suitable g 's, we are interested in very weak solutions of (29) of the form $u \in L^2(Q_T)$.

Firstly we must show that (29)₄ makes sense when $u \in L^2(Q_T)$ satisfies (29)₁₋₃ and, say, $g \in L^2(\Gamma_T)$. Let V_2 be the closure of \mathcal{V} in $H_0^2(\Omega)^2$, then $V_2 \subset H \subset V_2'$ with continuous injections and each space dense in the next one and, $\forall v \in L^2(0, T; \mathcal{V})$,

$$(30) \quad \frac{d}{dt}(u, v) = \langle \Delta u, v \rangle - \langle \nabla p, v \rangle = \langle u, \Delta v \rangle,$$

and by continuity, (30) holds for every $v \in L^2(0, T; V_2)$; and we conclude that

$$(31) \quad \frac{\partial u}{\partial t} \in L^2(0, T; V_2'),$$

and $u(0)$ makes sense, since u is a.e. equal to a continuous function from $[0, T]$ into V_2' .

A priori estimate

Our first result now will be an analogue of Lemma 2.

Lemma 3. *Assume that u, p, g and u_0 are sufficiently regular (e.g. $u \in L^2(0, T; H^2(\Omega)^2)$, $p \in L^2(0, T; H^1(\Omega))$, $u_0 \in H^1(\Omega)^2$), and satisfy (29). Then*

$$(32) \quad |u|_{L^2(0, T; L^2(\Omega)^2)} \leq c_2(|u_0|_{L^2(\Omega)^2} + |g|_{L^2(0, T; L^2(\Omega)^2)}),$$

where the constant c_2 depends only on Ω and T .

Proof. The proof is based again on a transposition argument as in Lemma 1.

We consider v, q solutions of the adjoint system

$$(33) \quad \begin{cases} -\frac{\partial v}{\partial t} - \Delta v + \nabla q = u & \text{in } Q_T, \\ \operatorname{div} u = 0 & \text{in } Q_T, \\ v = 0 & \text{on } \Gamma_T, \\ v(T) = 0, \end{cases}$$

and we write

$$(34) \quad \begin{aligned} & \int_{Q_T} u^2 dx dt \\ &= \int_{Q_T} u \left(-\frac{\partial v}{\partial t} - \Delta v + \nabla q \right) dx dt \\ &= \int_{\Omega} u_0 v(0) dx + \int_{Q_T} \left(\frac{\partial u}{\partial t} - \Delta u \right) v dx dt - \int_{\Gamma_T} g \left(\frac{\partial v}{\partial n} - nq \right) d\Gamma_T \\ &= \int_{\Omega} u_0 v(0) dx - \int_{Q_T} \nabla p \cdot v \, dQ_T - \int_{\Gamma_T} g \left(\frac{\partial v}{\partial n} - nq \right) d\Gamma_T \\ &= \int_{\Omega} u_0 v(0) dx - \int_{\Gamma_T} g \left(\frac{\partial v}{\partial n} - nq \right) d\Gamma_T \\ &\leq |u_0|_{L^2(\Omega)^2} |v(0)|_{L^2(\Omega)^2} + |g|_{L^2(0, T; L^2(\Gamma_T)^2)} \left| \frac{\partial v}{\partial n} - nq \right|_{L^2(0, T; L^2(\Gamma_T)^2)}. \end{aligned}$$

Now setting $s = t - T$ and writing $\hat{v}(s) = v(t)$, $\hat{u}(s) = u(t)$, we can rewrite (33) in the form

$$(35) \quad \frac{d\hat{v}}{ds} + A\hat{v} = \hat{u}, \quad \hat{v}(0) = 0,$$

where A is the abstract Stokes operator.

It is classical using a Galerkin method (see e.g. [58, Ch. II, Sec. 3 and Ch. IV, Sec. 9]) that the solution \hat{v} of (35) belongs to $L^\infty(0, T; V)$, $V = D(A^{1/2})$, and $d\hat{v}/ds$ belongs to $L^2(0, T; L^2(\Omega)^2)$: the necessary a priori estimate is formally obtained by taking the scalar product in $L^2(\Omega)^2$ of each side of (35) with $d\hat{v}/ds$. Then equation (35) shows that $A\hat{v}$ belongs also to $L^2(0, T; L^2(\Omega)^2)$. In addition there exists a constant c such that:

$$(36) \quad |A\hat{v}|_{L^2(0,T;L^2(\Omega)^2)} + \left| \frac{d\hat{v}}{ds} \right|_{L^2(0,T;L^2(\Omega)^2)} \leq c|\hat{u}|_{L^2(0,T;L^2(\Omega)^2)}.$$

Hence, returning to v and u :

$$(37) \quad |Av|_{L^2(0,T;L^2(\Omega)^2)} + \left| \frac{dv}{dt} \right|_{L^2(0,T;L^2(\Omega)^2)} \leq c|u|_{L^2(0,T;L^2(\Omega)^2)}.$$

As observed in Remark 3, the Stokes problem for the domain Ω that we consider enjoys the $H^2 - H^1$ regularity. This means that $D(A) \subset H^2(\Omega)^2$ and the corresponding q belongs to $H^1(\Omega)$.

Finally for (33):

$$(38) \quad |v|_{L^2(0,T;H^2(\Omega)^2)} + |q|_{L^2(0,T;H^1(\Omega))} + \left| \frac{dv}{dt} \right|_{L^2(0,T;L^2(\Omega)^2)} \leq c|u|_{L^2(0,T;L^2(\Omega)^2)}.$$

Implementing this inequality in (35), the lemma follows.

The trace issues

We next deal with the trace issues.

Let (u,p) be the solutions of the following system:

$$(39) \quad \begin{cases} \frac{\partial u}{\partial t} - \Delta u + \nabla p = 0 & \text{in } Q_T, \\ \operatorname{div} u = 0 & \text{in } Q_T \\ u(0) = 0 & \text{in } \Omega. \end{cases}$$

Then, in relation with (29) we consider the set

$$\mathcal{F}(Q_T) := \{u \in L^2(Q_T)^2 \text{ s.t. } \exists p \in \mathcal{D}'(Q_T) \text{ and } u \text{ satisfies (39)}\}.$$

Recall that we have shown in (29)-(32) that if $u \in L^2(Q_T)^2$ satisfies (39)₁₋₂ then u is a.e. equal to a continuous function from $[0, T]$ into V'_2 . Hence (39)₃ makes sense and the definition of $\mathcal{F}(Q_T)$ is valid. Furthermore using the current theory [47] as in the stationary case, we see that $\mathcal{F}(Q_T)$ is closed in Q_T . Indeed if (39) holds for a sequence $u_n \in L^2(Q_T)^2$, $p_n \in \mathcal{D}'(Q_T)$, and $u_n \rightarrow u$ in $L^2(Q_T)^2$, then ∇p_n converges to $F = \Delta u - \partial u / \partial t$ in $\mathcal{D}'(Q_T)$ and necessarily $F = \nabla p$ for some $p \in \mathcal{D}'(Q_T)$, so that (39) holds for u and p . Similarly $\operatorname{div} u_n = 0$ converges to $\operatorname{div} u$ in $\mathcal{D}'(Q_T)$ so that $\operatorname{div} u = 0$ and the trace $u_n(0)$ being continuous, it converges to $u(0)$ in V'_2 . Hence (39) holds and $u \in \mathcal{F}(Q_T)$.

Concerning the trace on Γ_T of a function u in $\mathcal{F}(Q_T)$, we first observe that the normal component of u , $\gamma_n(u) = u \cdot n|_{\Gamma_T}$ is defined and belongs to $L^2(0, T; H^{-1/2}(\Gamma_T)^2)$, according to a standard trace result in the Navier-Stokes theory [59]. So the issue is to define the tangential component of u on Γ_T , $\gamma_\tau(u)$. As in the stationary case, we will define $\gamma_\tau(u)$ by its duality with the trace on Γ_T of a suitable function v . More precisely consider

$$\mathcal{X}_2(Q_T) = \{v \in L^2(0, T; H^2(\Omega)^2), \operatorname{div} v = 0, v = 0 \text{ on } \Gamma_T\},$$

and the subspace

$$\mathcal{Y}_2(Q_T) = \{v \in L^2(0, T; H^2(\Omega)^2), \operatorname{div} v = 0, \\ \frac{\partial v}{\partial t} \in L^2(0, T; L^2(\Omega)^2), v = 0 \text{ on } \Gamma_T, v(T) = 0\}.$$

Using the lifting operator R from Corollary 1, we see that γ_1 is a surjective operator from $\mathcal{X}_2(Q_T)$ onto $L^2(0, T; H_\tau^{1/2}(\Gamma)^2)$. Also it is elementary to see that $\mathcal{Y}_2(Q_T)$ is dense in $\mathcal{X}_2(Q_T)$ equipped with the norm $|v|_{L^2(0, T; H^2(\Omega)^2)}$ so that the traces $\gamma_1(v)$ for $v \in \mathcal{Y}_2(Q_T)$ are dense in $L^2(0, T; H_\tau^{1/2}(\Gamma)^2)$.

Now for $g_1 \in \gamma_1(\mathcal{Y}_2(Q_T))$ let v be one of the functions in $\mathcal{Y}_2(Q_T)$ such that $\gamma_1 v = \partial v / \partial n|_{\Gamma_T} = g_1$. For u satisfying (39), consider the expression

$$(40) \quad \mathcal{L}_u(g_1) = - \int_{Q_T} u \left(\frac{\partial v}{\partial t} + \Delta v \right) dxdt.$$

For u and v smooth we have by integration by parts, and using Green's formula,

$$\begin{aligned} \mathcal{L}_u(g_1) &= \int_{Q_T} v \left(\frac{\partial u}{\partial t} - \Delta u \right) dxdt - \int_{\Gamma_T} u \frac{\partial v}{\partial n} d\Gamma_T \\ &= - \int_{Q_T} v \nabla p dxdt - \int_{\Gamma_T} u \frac{\partial v}{\partial n} d\Gamma_T \\ &= - \int_{\Gamma_T} u \frac{\partial v}{\partial n} d\Gamma_T = - \int_{\Gamma_T} u g_1 d\Gamma_T. \end{aligned}$$

Hence the expression (40) has the potential to define and characterize the tangential components of u in $L^2(0, T; H_\tau^{-1/2}(\Gamma_\tau))$ since the g under consideration are dense in $L^2(0, T; H_\tau^{1/2}(\Gamma_T)^2)$.

Our next task is to show that the expression $\mathcal{L}_u(g_1)$ is independent of the choice of $v \in \mathcal{Y}_2(Q_T)$ such that $\frac{\partial v}{\partial n} = g$ on Γ_T . Consider two such functions v_1, v_2 and their difference $v = v_1 - v_2$. We must show that

$$(41) \quad \int_{Q_T} u \left(\frac{\partial v}{\partial t} + \Delta v \right) dxdt = 0,$$

when $u \in \mathcal{F}(Q_T)$ and $v \in \mathcal{Y}_2(Q_T)$ satisfies $\partial v / \partial n = 0$ on Γ_T . Then such a v belongs to $L^2(0, T; H_0^2(\Omega)^2)$, that is $L^2(0, T; \tilde{X}_2(\Omega))$, $\tilde{X}_2(\Omega)$ as in (16). For v in $L^2(0, T; \mathcal{V})$, the expression (41) vanishes because it is equal to

$$\begin{aligned} &< - \frac{\partial u}{\partial t} + \Delta u, v >_{\mathcal{D}'(Q_T), \mathcal{D}(Q_T)} \\ &= < \nabla p, v >_{\mathcal{D}'(Q_T), \mathcal{D}(Q_T)} = 0. \end{aligned}$$

Since we showed in Lemma 2 that \mathcal{V} is dense in $\tilde{X}_2(\Omega)$, we infer that $L^2(0, T; \mathcal{V})$ is dense in $L^2(0, T; \tilde{X}_2(\Omega))$ and (41) holds for any v in $\mathcal{Y}_2(Q_T)$ satisfying $\partial v / \partial n = 0$ on Γ_T .

We then have the analogue of Theorem 2.

Theorem 4. *Under the hypotheses of Theorem 1 (Γ of class \mathcal{C}^2 or of polygonal type), there exists a linear continuous operator $\gamma_\tau \in \mathcal{L}(\mathcal{F}(Q_T), L^2(0, T; H_\tau^{-1/2}(\Gamma)^2))$ such that*

$$\gamma_\tau u = u \cdot \tau|_{\Gamma_T} \text{ for every } u \in \mathcal{F}(Q_T) \cap \mathcal{C}^2(\bar{Q}_T).$$

The following generalized Stokes formula is valid for all $u \in \mathcal{F}(Q_T)$ and $g_1 \in \gamma_1(\mathcal{Y}_2(Q_T)) \subset L^2(0, T; H^{-1/2}(\Gamma)^2)$:

$$(42) \quad \langle \gamma_\tau u, g_1 \rangle = \int_{Q_T} u \left(\frac{\partial v}{\partial t} + \Delta v \right) dxdt,$$

where v is any function of $\mathcal{Y}_2(Q_T)$ such that $\gamma_1(v) = g_1$.

All statements have been proven or are proven as in Section 1.

The existence and uniqueness theorem

Theorem 5. *We assume that Ω is of class C^2 or is of polygonal type and that g is given in $L^2(0, T; L^2(\Gamma)^2)$ satisfying (18) for a.e. $t \in [0, T]$.*

Then there exists a unique function $u \in L^2(Q_T)^2$ satisfying (29) for some $p \in \mathcal{D}'(Q_T)$.

Proof. We approach g by a sequence $g_j \in L^2(0, T; H^{3/2}(\Gamma)^2)$ as in (19), where g_j converges to g in $L^2(0, T; H^{-1/2}(\Gamma)^2)$ as $j \rightarrow \infty$. For each j we find, by [56], [57], $u_j, p_j \in L^2(0, T; H^2(\Omega)^2) \times L^2(0, T; H^1(\Omega))$ satisfying (29). The estimates provided by Lemma 3 show that the sequence u_j is bounded in $L^2(Q_T)^2$. Therefore u_j contains a subsequence weakly convergent in $L^2(Q_T)^2$ to some limit u , and u satisfies (29) for some $p \in \mathcal{D}'(Q_T)$, thanks to [47].

We are left with the uniqueness, that is proving that $u = 0$ when $u \in \mathcal{F}(Q_T)$ satisfies (29) with $g = 0$. We introduce the solution v of the adjoint system as in (33). Then $v \in \mathcal{Y}_2(Q_T)$ and

$$\begin{aligned} \int_{Q_T} |u|^2 dxdt &= \int_{Q_T} u \left(-\frac{\partial v}{\partial t} - \Delta v + \nabla q \right) dxdt \\ &= \text{(using (42) with } \gamma_1(u) = 0 \text{)} \\ &= \int_{Q_T} u \nabla q dxdt = \int_0^T \int_\Omega u \nabla q dxdt, \end{aligned}$$

and this last expression vanishes as in (21).

The theorem is proved.

Part 2. Numerical simulations

The second part of this article is devoted to the numerical study of the Stokes solutions in a square. This is the well known lid-driven cavity problem. Taking advantage of the theoretical study in Part 1 we will see how the use of the finite element method together with the regularization of the boundary velocity can help solving the issues due to the corners.

5. Regularized Stokes problem

As a numerical illustration, we would like to present a regularization treatment on the lid driven cavity problem:

$$(43) \quad \begin{cases} -\Delta u + \nabla p = 0 \text{ in } \Omega, \\ \operatorname{div} u = 0 \text{ in } \Omega, \\ u = g \text{ on } \Gamma. \end{cases}$$

In this case Ω is the square $(-1, 1) \times (-1, 1)$ and $\Gamma = \partial\Omega$; $g = (0, 0)$ at $x = -1, 1$ and $y = 0$, and $g = (1, 0)$, at $y = 1$; the discontinuities of g produce singularities and vortices at the corners of the square domain $(-1, 1)$ and $(1, 1)$.

We call ε as the regularization parameter. According to the regularization method proposed in Section 3, we approximate g by g_ε , the regularized Dirichlet boundary condition, which is identical to g except for the first component which is equal to

$$(44) \quad 1 - \sigma(x)e^{-(1+x)/\varepsilon} - \sigma(-x)e^{-(1-x)/\varepsilon}$$

on the side $y = 1$, where σ is chosen less smooth (\mathcal{C}^2) than in (23), that is, a smoothstep function

$$(45) \quad \sigma(x) = \begin{cases} 1, & -1 \leq x \leq -\frac{1}{2} \\ 6(\frac{1}{2} - x)^5 - 15(\frac{1}{2} - x)^4 + 10(\frac{1}{2} - x)^3, & -\frac{1}{2} \leq x \leq \frac{1}{2} \\ 0, & \frac{1}{2} \leq x \leq 1. \end{cases}$$

Therefore, both g and g_ε satisfy the necessary conditions

$$(46) \quad \int_{\Gamma} g \cdot n \, d\Gamma = \int_{\Gamma} g_\varepsilon \cdot n \, d\Gamma = 0,$$

where n is the outward normal vector alongside Γ . It is clear that g_ε converges to g in $L^2(\Gamma)^2$ as $\varepsilon \rightarrow 0$. In view of Theorem 3, there exists a unique solution (u, p) to the problem (43) with $u \in L^2(\Omega)^2$, and a unique solution $(u_\varepsilon, p_\varepsilon)$ to the problem (43) with g replaced by g_ε , and $u_\varepsilon \in L^2(\Omega)^2$; as usual the uniqueness of p, p_ε is meant up to the addition of a constant. In addition, when $\varepsilon \rightarrow 0$,

$$(47) \quad g_\varepsilon \rightarrow g \text{ in } L^2(\Gamma)^2,$$

and consequently

$$(48) \quad u_\varepsilon \rightarrow u \text{ in } L^2(\Omega)^2.$$

6. Discretization of the Stokes problem and its regularized version

In this section, we introduce the discretized version of both the original Stokes problem and its regularized version. In fact, the two problems can be written in the same discrete form despite a superscription ε . First, we state the weak formulation of the Stokes problem. We define the continuous bilinear forms $a : H^1(\Omega)^2 \times H^1(\Omega)^2 \rightarrow \mathbb{R}$, and $b : H^1(\Omega)^2 \times L^2(\Omega) \rightarrow \mathbb{R}$ so that

$$(49) \quad a(u, v) := \int_{\Omega} \nabla u \cdot \nabla v = \sum_{i=1}^2 \int_{\Omega} \nabla u_i \cdot \nabla v_i$$

$$(50) \quad b(u, q) := - \int_{\Omega} q \nabla \cdot u.$$

Therefore the weak formulation of the Stokes problem (43) can be written as follows:

Find $u \in H^1(\Omega)^2$ and $p \in L^2(\Omega)$, $u|_{\Gamma} = g$, such that

$$(51) \quad \begin{aligned} a(u, v) + b(v, p) &= 0 \quad \text{for all } v \in H_0^1(\Omega)^2; \\ b(u, q) &= 0 \quad \text{for all } q \in L^2(\Omega). \end{aligned}$$

To discretize the Stokes equations, we first introduce a quadrilateral finite element partition \mathcal{M}_h consisting of squares of area h^2 on domain Ω . We use different

types of finite elements construction on \mathcal{M}_h . The following plot in Figure 1 is an illustration of a $Q_2 - P_1$ mixed finite elements partition.

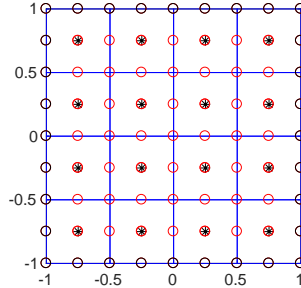


FIGURE 1. $Q_2 - P_1$ finite element subdivisions, where \circ are velocity nodes and $*$ are pressure nodes.

We will use the example of $Q_2 - P_1$ finite element method to describe the discretized problems. Here the velocity nodes are approximated on each rectangular element using Q_2 functions of the form $(ax^2 + bx + c)(dy^2 + ey + f)$, which are linear combinations of the nine terms $1, x, y, x^2, xy, y^2, x^2y, xy^2, x^2y^2$. The pressure nodes are approximated on each rectangular element using P_1 functions, which are linear combinations of the terms $1, \frac{2}{h}(x - \bar{x})$ and $\frac{2}{h}(y - \bar{y})$, where (\bar{x}, \bar{y}) are the coordinates of the centroid of the element. Therefore, we define the following finite dimensional spaces on partition \mathcal{M}_h :

$$(52) \quad X^h(\Omega)^2 := \{v \in C^0(\Omega)^2; v|_E \in Q_2 \text{ for all } E \in \mathcal{M}_h\},$$

$$(53) \quad X_0^h(\Omega)^2 := \{v \in C^0(\Omega)^2, v = 0 \text{ on } \partial\Omega; v|_E \in Q_2 \text{ for all } E \in \mathcal{M}_h\},$$

$$(54) \quad M^h(\Omega) := \{q \in C^0(\Omega); q|_E \in P_1 \text{ for all } E \in \mathcal{M}_h\}.$$

The formal aspects of the finite elements discretization of the Stokes equations (43) are defined using two finite dimensional spaces $X_0^h(\Omega)^2 \subset H_0^1(\Omega)^2$ and $M^h(\Omega) \subset L^2(\Omega)$, which is commonly identified as a mixed finite element approximation method. Specifically for the $Q_2 - P_1$ method, given the velocity solution space $X^h(\Omega)^2$ as defined in (52) and the pressure solution space $M^h(\Omega)$ as defined in (54), the discrete problem can be written as follows:

Find $u_h \in X^h(\Omega)^2$ and $p_h \in M^h(\Omega)$ with $u_h|_\Gamma = g_h$ such that

$$(55) \quad \begin{aligned} a(u_h, v_h) + b(v_h, p_h) &= 0 \quad \text{for all } v_h \in X_0^h(\Omega)^2; \\ b(u_h, q_h) &= 0 \quad \text{for all } q_h \in M^h(\Omega). \end{aligned}$$

Here g_h is a discretization of g consistent with the mesh.

The discrete problem of the regularized Stokes problem is the same as (55) except for replacing u_h by u_h^ε , p_h by p_h^ε and g_h by g_h^ε . Here g_h^ε is a discretization of g_h consistent with the mesh.

7. Effectiveness of the regularization method

The purpose of this section is to explore the effectiveness of our proposed regularization method and its relevance to the regularization parameter ε . According to the regularized Dirichlet boundary condition g^ε proposed in (44) and (45), we know it is a second order smooth “bump” function. It is fair to expect that the effectiveness of the regularization method depends on different choices of ε . More specifically speaking, a smaller ε may not always be a better choice. This is because $g^\varepsilon \rightarrow g$ when $\varepsilon \rightarrow 0$, hence we are almost solving the original discrete Stokes problem if the bump up or bump down at the corners $(-1, 1)$ and $(1, 1)$ happens within the unit difference in the horizontal direction.

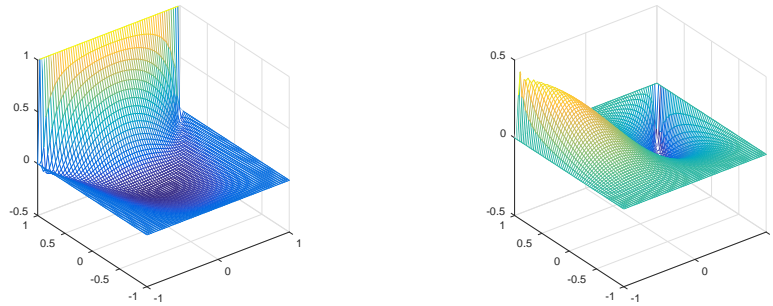
(a) The first velocity component u_1 (b) The second velocity component u_2

FIGURE 2. Velocity plots of the Stokes problem with mesh size = $2^6 \times 2^6$.

To determine an optimal choice of ε , we need to discuss the behavior of the velocity and pressure solutions under a fixed mesh size. In this section, we adopt a quadrilateral finite element partition \mathcal{M}_h consisting of square elements of area h^2 on the domain Ω . In consideration of the balance of illustration purpose and computation time, we choose $h = 2^{-6}$. Moreover, we implement a $Q_1 - P_0$ mixed finite element approximation.

First, we compare the results between the Stokes problem and its regularized version in the following plots. In consideration of showing the effectiveness of the regularization method, we choose a not so small value, namely $\varepsilon = 0.1$, to give a visually smooth Dirichlet boundary condition. The Figures 2 to 7 provide an intuitive view of effectiveness of the regularization method: Figure 2 and 3 plot both components of velocity solutions u of the Stokes problem and u^ε of the problem respectively; Figure 4 and 5 plot contour views of u and u^ε ; Figure 6 and 7 plot the stream lines and pressure solutions of both the Stokes problem and its regularized version respectively.

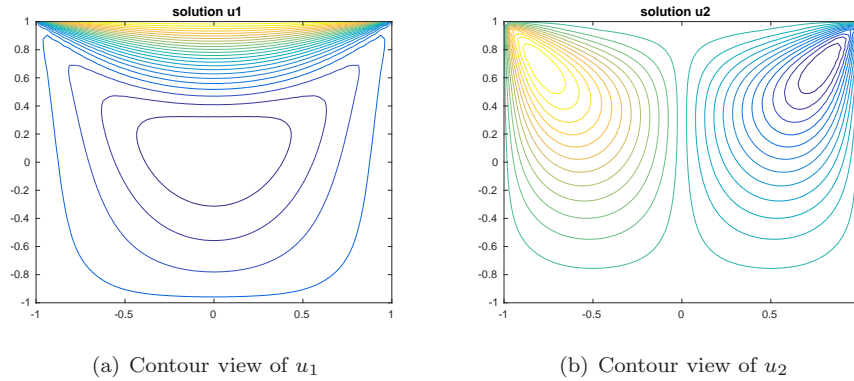


FIGURE 5. Contour views of the velocity solutions of the regularized Stokes problem with mesh size $= 2^6 \times 2^6$.

From the contour views of the velocity solutions plotted in Figures 4 and 5, even though it is not significant, we can still see that the contour lines near the corners $(-1, 1)$ and $(1, 1)$ of the solutions to the regularized Stokes problem have less sharp corners than those of the solutions to the original Stokes problem.

We next show the stream and pressure solutions plots in Figures 6 and 7. The vortices observed from the stream solution of the regularized Stokes problem near the corners $(-1, 1)$ and $(1, 1)$ are less severe than those from the original Stokes problem. By comparing the plots of the pressure solutions between the two systems, they imply that the regularized Stokes pressure solution has sharp spikes as low as half of those from the original Stokes problem, in the vicinity of the two corners $(-1, 1)$ and $(1, 1)$. A higher pressure causes the incompressible fluid flows at a higher velocity, which pushes the stream harder to the corners and produces singularities.

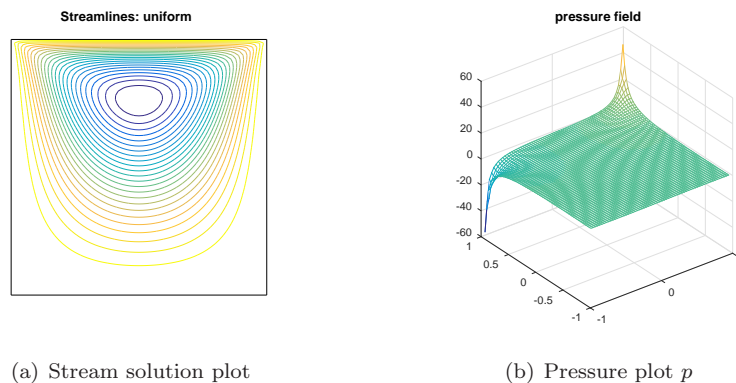
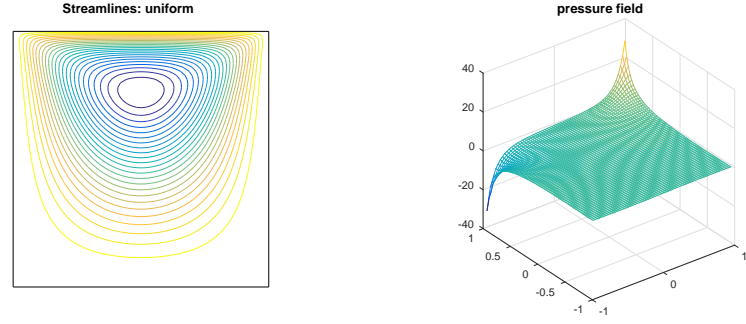


FIGURE 6. Contour view of the stream solution and 3-D view of the pressure solution to the original Stokes problem with mesh size $= 2^6 \times 2^6$.



(a) Stream solution plot

 (b) Pressure plot p

 FIGURE 7. Contour view of the stream solution and 3-D view of the pressure solution to the regularized Stokes problem with mesh size $= 2^6 \times 2^6$.

We introduce here a combined symmetric bilinear form

$$(56) \quad B((u, p); (v, q)) := a(u, v) + b(v, p) + b(u, q).$$

Therefore, the weak formulation (51) can be rewritten in the following form: Find $(u, p) \in H^1(\Omega)^2 \times L^2(\Omega)$, $u|_{\Gamma} = g$, such that

$$(57) \quad B((u, p); (v, q)) = 0, \quad \text{for all } (v, q) \in H_0^1(\Omega)^2 \times M^h(\Omega).$$

We then define the two elementwise interior residual estimators by

$$(58) \quad \mathbf{R}_T := (\nabla^2 u_h - \nabla p_h)|_T,$$

and

$$(59) \quad R_T := (\nabla \cdot u_h)|_T.$$

Moreover, the inter-element stress jump across the edge E adjoining elements T and S can be defined as

$$(60) \quad \mathbf{R}_E := \{(\nabla u_h - p_h \mathbf{I})|_T - ((\nabla u_h - p_h \mathbf{I})|_S)\} n_{E,T},$$

where \mathbf{I} is 2×2 identity matrix. Together with the Dirichlet boundary edges, we define the elementwise boundary residual estimator

$$(61) \quad \mathbf{R}_E^* := \begin{cases} \frac{1}{2} \{(\nabla u_h - p_h \mathbf{I})|_T - ((\nabla u_h - p_h \mathbf{I})|_S)\} n_{E,T}, & \text{when } E \text{ is an inter-element edge,} \\ 0, & \text{when } E \text{ is on the Dirichlet boundary.} \end{cases}$$

Then we define the discretization errors $(\mathbf{e}, \epsilon) := (u - u_h, p - p_h) \in H_0^1(\Omega)^2 \times L^2(\Omega)$ that can be characterized by

$$\begin{aligned}
 & \sum_{T \in \mathcal{M}} \left\{ (\nabla \mathbf{e}, \nabla v)_T - (\epsilon, \nabla \cdot v)_T \right\} \\
 &= \sum_{T \in \mathcal{M}} \left\{ \left\{ (\nabla u, \nabla v)_T - (p, \nabla \cdot v)_T \right\} - \left\{ (\nabla u_h, \nabla v)_T - (p_h, \nabla \cdot v)_T \right\} \right\} \\
 (62) \quad &= \sum_{T \in \mathcal{M}} \left\{ \left\{ B((u, p); (v, q)) - b(u, q) \right\} - \left\{ B((u_h, p_h); (v, q)) - b(u_h, q) \right\} \right\} \\
 &= \sum_{T \in \mathcal{M}} \left\{ B((u - u_h, p - p_h); (v, q)) - b(e, q) \right\} \\
 &= \sum_{T \in \mathcal{M}} \left\{ (R_T, v)_T - \sum_{E \in \mathcal{E}(T)} \langle R_E^*, v \rangle_E \right\} - \sum_{T \in \mathcal{M}} (q, \nabla \cdot e) + \sum_{T \in \mathcal{M}} (R_T, q)_T.
 \end{aligned}$$

Now we introduce (and then we compare) the local and global error estimators between the original and the regularized Stokes problems which read, respectively, as follows:

$$\begin{aligned}
 (63) \quad \eta_T^2 &:= \|\nabla^2 e_T\|_T^2 + \|\epsilon_T\|_T^2 \\
 &= \|\nabla^2 e_T\|_T^2 + \|\nabla \cdot u_h\|_T^2,
 \end{aligned}$$

and

$$(64) \quad \eta := \left(\sum_{T \in \mathcal{T}_h} \eta_T^2 \right)^{1/2},$$

where u_h is defined by (55), and e, ϵ are defined by (62). This comparison provides a substantial view of the effectiveness of the regularization method. Let η_T and η_T^ϵ denote the element-wise error estimators and η and η^ϵ denote the global error estimators. Figure 8 gives graphs of η_T and Figure 9 gives graphs of η_T^ϵ .

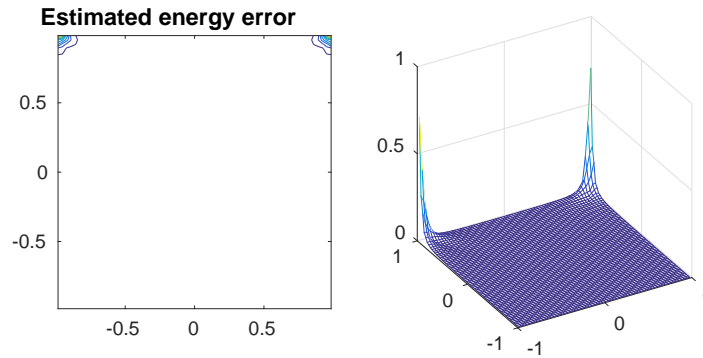


FIGURE 8. Element-wise energy estimator η_T of the original Stoke problem.

It is not surprising that the maximum values happen near both of the corners $(-1, 1)$ and $(1, 1)$, appearing on the local error estimator plot are the two positive spikes at these two corners. From the calculated element-wise local error estimator, we see that the regularization method reduces the maximum of the local energy estimators from 0.7091 to 0.1029, which is approximately $1/7$ as low as those from the original Stokes equations.

Finally, we compare the global error estimator. According to the simulation results from the two Stokes problems, $\eta = 1.3992$ and $\eta^\varepsilon = 0.4202$, the global energy error estimate is rapidly decreased.

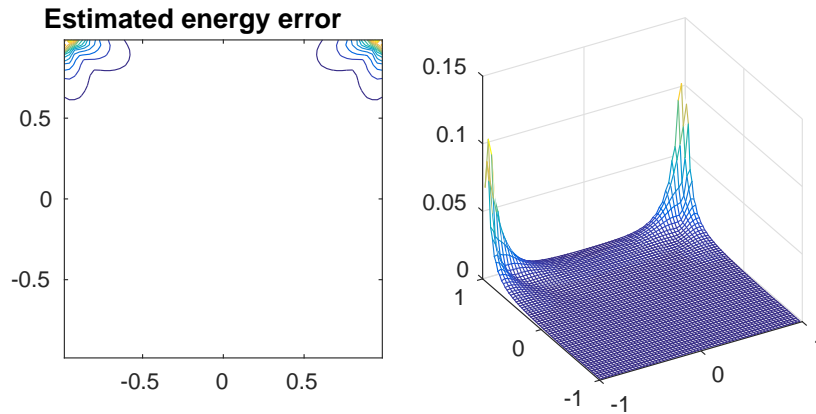


FIGURE 9. Element-wise energy estimator η_T^ε of the regularized Stokes problem.

The next step is to find, an optimized ε , on the same mesh grid size of $2^6 \times 2^6$, such that the a posteriori error is reduced, while the regularized boundary condition is close to the original. Here we need to introduce a utility function in order to set a measure to quantify the effectiveness of the regularization method. Since the global error estimator η only gives an estimate of the difference between the actual solution and the simulated solution, it is not sufficiently robust to determine the effectiveness of the regularization method. In fact, when $\varepsilon = 0.5$, the solution is very different from our original problem. Hence, it is meaningless to study a regularized Stokes problem with such a large ε . We give the plots of the velocity solutions to the regularized Stokes problem with $\varepsilon = 0.5$ as in Figure 10.

The following Figure 11 plots η depending on a set of ε ranging from 0 to 0.6. With a larger value of ε , we have less severe bumps near the vicinity of the two corners $(-1, 1)$ and $(1, 1)$. Therefore, we can see from the results of Figure 11 below,

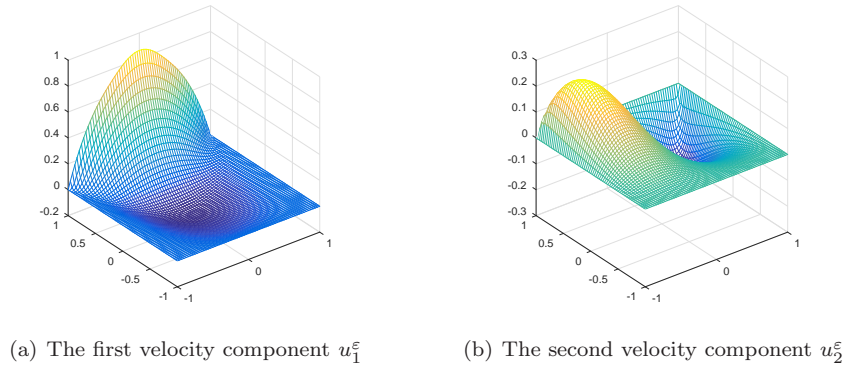


FIGURE 10. Velocity plots of the regularized Stokes problem with $\varepsilon = 0.5$.

the a posteriori global error estimates caused by the singularities near these two corners decrease as ε increases. It lacks evidence of the existence of an optimal ε .

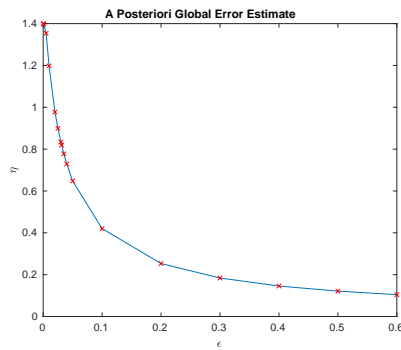


FIGURE 11. The global energy estimator η^ε decreases as ε increases.

Therefore the discussion above implies that the a posteriori global error estimate is not helpful to determine the optimal ε . In this consideration, we introduce the following norm to measure the difference between the original solution u and the regularized solution u^ε . Define

$$(65) \quad \xi = |u - u^\varepsilon|_{X^h(\Omega)}^2.$$

We can find the value of ξ by solving the following system, i.e. subtracting the Stokes problem (43) from its regularized version gives

$$(66) \quad \begin{cases} -\Delta(u - u^\varepsilon) + \nabla(p - p^\varepsilon) = 0 \text{ in } \Omega, \\ \operatorname{div}(u - u^\varepsilon) = 0 \text{ in } \Omega, \\ u = g - g^\varepsilon \text{ on } \Gamma. \end{cases}$$

The solution of the problem above gives ξ to measure the difference between the Stokes problem and its regularized version. Moreover, we can measure the difference between the simulated solution of the regularized Stokes problem and the actual

solution of the original Stokes problem by observing that

$$\begin{aligned}
 |u_h^\varepsilon - u|_{X^h(\Omega)^2}^2 &= |u_h^\varepsilon - u^\varepsilon + u^\varepsilon - u|_{X^h(\Omega)^2}^2 \\
 (67) \qquad \qquad \qquad &\leq 2(|u_h^\varepsilon - u^\varepsilon|_{X^h(\Omega)^2}^2 + |u^\varepsilon - u|_{X^h(\Omega)^2}^2) \\
 &\leq 2(\eta^2 + \xi^2).
 \end{aligned}$$

Therefore, we can drop the constant multiplier and define the regularization effectiveness θ as

$$(68) \qquad \qquad \qquad \theta = (\eta^2 + \xi^2)^{1/2}$$

such that, θ implies both the a posteriori error estimate from the numerical simulation and the difference between the original Stokes and its regularized version. We now use θ to measure the effectiveness of our regularization method. It is natural to conclude that the smaller θ is, the more effective the regularization method is.

The Figure 12 plots θ corresponding to a set of ε ranging from 0 to 0.6. We can see that when ε increases, θ first decreases fast near 0, then increases as ε gets larger. When ε is approximately $2^{-5} = 2h$, which is about the same size as two element patches, θ is minimized. The table of calculated a posteriori errors with some selected choices of ε follows:

TABLE 1. Table of regularization effectiveness θ with selected ε .

| ε | η^ε | θ |
|---------------|--------------------|--------------|
| 0 | 1.3992166632 | 1.3992166632 |
| 0.001 | 1.3992164888 | 1.3992164888 |
| 0.005 | 1.3535723177 | 1.3556063758 |
| 0.01 | 1.1977452192 | 1.2424769311 |
| 0.02 | 0.9773442412 | 1.1798006234 |
| 0.025 | 0.8997346841 | 1.1753470829 |
| 0.03 | 0.8342184564 | 1.1755834200 |
| 2^{-5} | 0.8193522005 | 1.1760985764 |
| 0.035 | 0.7778433423 | 1.1784442289 |
| 0.04 | 0.7287624950 | 1.1830037818 |
| 0.05 | 0.6475161959 | 1.1951386669 |
| 0.1 | 0.4201681138 | 1.2642598827 |
| 0.2 | 0.2531435181 | 1.3585403309 |
| 0.3 | 0.1839190614 | 1.4196779532 |
| 0.4 | 0.1456914817 | 1.4662024339 |
| 0.5 | 0.1213483106 | 1.5037638424 |
| 0.6 | 0.1044166356 | 1.5348455531 |

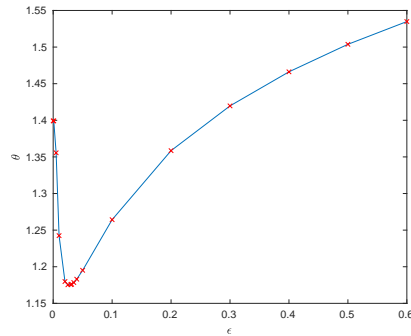


FIGURE 12. Plot of θ depend on ε .

We come to the conclusion that the regularization method is most effective when $\varepsilon \approx 2h$.

8. Advantage of the regularization method

The previous section focuses on finding the most effective regularization method on a grid of given mesh size. Besides improved a posteriori error estimates, the regularization method brings more advantages. In order to explore these benefits, we first fix a reasonable ε . Based on the observations from the previous section, we choose $\varepsilon = 0.1$, which leads to a solution close enough but not numerically identical to the original one.

Now we simulate both the original and regularized Stokes problems using four popular mixed finite element schemes, namely $Q_1 - Q_1$, $Q_1 - P_0$, $Q_2 - Q_1$ and $Q_2 - P_1$ as illustrations. For each fixed mesh size, for example on a $2^4 \times 2^4$ grid, all the finite element scheme have the same velocity nodes, i.e. 17 in each direction. The number of pressure nodes varies based on the scheme.

TABLE 2. A Posteriori estimates on various grids.

| ε | Finite Element Method | $2^4 \times 2^4$ | $2^5 \times 2^5$ | $2^6 \times 2^6$ | $2^7 \times 2^7$ | $2^8 \times 2^8$ |
|---------------|-----------------------|------------------|------------------|------------------|------------------|------------------|
| 0 | $Q_1 - Q_1$ | 1.445234 | 1.446634 | 1.446958 | 1.447031 | 1.447049 |
| | $Q_1 - P_0$ | 1.396908 | 1.398758 | 1.399216 | 1.399325 | 1.399351 |
| | $Q_2 - Q_1$ | 2.353259 | 2.353237 | 2.353045 | 2.352993 | 2.352981 |
| | $Q_2 - P_1$ | 1.075365 | 1.074823 | 1.074466 | 1.074365 | 1.074341 |
| | $Q_1 - Q_1$ | 0.879755 | 0.596736 | 0.370109 | 0.216801 | 0.122542 |
| 0.1 | $Q_1 - P_0$ | 0.895467 | 0.646189 | 0.420168 | 0.253920 | 0.146491 |
| | $Q_2 - Q_1$ | 1.551221 | 0.916437 | 0.483511 | 0.245228 | 0.123041 |
| | $Q_2 - P_1$ | 0.757472 | 0.478988 | 0.264134 | 0.136427 | 0.068842 |

From the table above, the top part with $\varepsilon = 0$ are the a posteriori error estimates for the original Stokes problem; the bottom part with $\varepsilon = 0.1$ are the a posteriori error estimates for the regularized Stokes problem.

Now according to the Table 2 above and Figure 13 below, we can see the main advantage of adopting a regularization method. The a posteriori energy estimate of the original Stokes problem keeps at the same level without much noticeable differences between coarser and finer grids, i.e. a finer mesh grid cannot improve the a posteriori error estimates. However, with the regularized system, the a posteriori error estimates decreases as the mesh grid gets finer.

The reason is as follows. With the original system, the discontinuities at both corners $(-1, 1)$ and $(1, 1)$ always happen within a single element patch at each

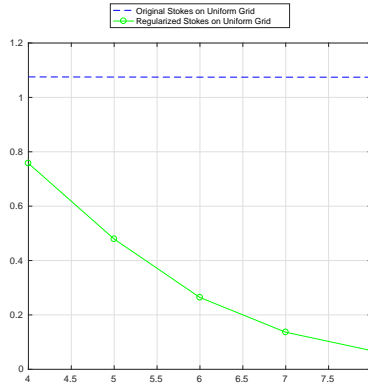


FIGURE 13. Plot of a posteriori error estimates with $Q_2 - P_1$.

corner. It maintains the elementwise energy estimates η_T at a constant level, which has a dominant impact on the global error estimate η . On the other hand, with the regularized system, even ε is very small, the boundary is always second order smooth. We can always find a mesh fine enough, such that the “bump” near the two top corners can be distributed into several element patches. Therefore both elementwise and global a posteriori error estimates are reduced.

The experiments above guarantee that with a fixed ε we can get a better approximation with a finer mesh regardless of the computational time.

9. Experiments on stretched grids

According to the results above, we consider to use stretched mesh grids to reduce the a posteriori error estimates without increasing the computational time.

As a starting point, we introduce a stretched mesh grid consisting of rectangles of dimension $h \times k$, where both h and k are decreasing from the center to all four edges $x = \pm 1$ and $y = \pm 1$. The following Figure 14 is an example of $Q_2 - P_1$ finite element subdivision on a $2^3 \times 2^3$ stretched mesh grid. The circles \circ are velocity nodes and the $*$ stand for centroid pressure nodes.

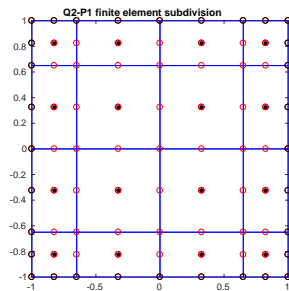


FIGURE 14. Plot of $Q_2 - P_1$ finite element subdivision on a $2^3 \times 2^3$ stretched mesh grid.

Then we again fix $\varepsilon = 0.1$ to make sure the results are comparable to those on the uniform mesh grids from the previous section. We also use the same mixed

finite element methods $Q_1 - Q_1$, $Q_1 - P_0$, $Q_2 - Q_1$ and $Q_2 - P_1$ in this numerical experiment and the results are as follows.

From the table below, the top half part with $\varepsilon = 0$ gives the a posteriori error estimates for the original Stokes problem; the bottom half part with $\varepsilon = 0.1$ gives the a posteriori error estimates for the regularized Stokes problem.

TABLE 3. Posteriori estimates on various grids.

| ε | Finite Element Method | $2^4 \times 2^4$ | $2^5 \times 2^5$ | $2^6 \times 2^6$ | $2^7 \times 2^7$ | $2^8 \times 2^8$ |
|---------------|-----------------------|------------------|------------------|------------------|------------------|------------------|
| 0 | $Q_1 - Q_1$ | 1.450230 | 1.448173 | 1.446205 | 1.445683 | 1.445873 |
| | $Q_1 - P_0$ | 1.503844 | 1.473941 | 1.442801 | 1.422594 | 1.411408 |
| | $Q_2 - Q_1$ | 2.298074 | 2.296589 | 2.310039 | 2.324835 | 2.335895 |
| | $Q_2 - P_1$ | 1.204518 | 1.144282 | 1.110241 | 1.093193 | 1.084458 |
| 0.1 | $Q_1 - Q_1$ | 0.556979 | 0.279458 | 0.134037 | 0.064728 | 0.032229 |
| | $Q_1 - P_0$ | 0.772454 | 0.441244 | 0.234534 | 0.123222 | 0.065335 |
| | $Q_2 - Q_1$ | 0.847015 | 0.283549 | 0.092135 | 0.030159 | 0.009947 |
| | $Q_2 - P_1$ | 0.536132 | 0.189310 | 0.060319 | 0.019062 | 0.006098 |

We come to the following conclusions. By comparing the top half of Tables 2 and 3, we can see that a finer stretched mesh grid cannot improve a posteriori error estimates of the original Stokes problem. On the other hand, according to the bottom half of Tables 2 and 3, the a posteriori error estimates are reduced a lot with stretched mesh grids. Using the finite element method $Q_2 - P_1$ as an example, we plot the errors in Figure 14. The top dash curve are the a posteriori error estimates from the original Stokes equations on the stretched grids; the middle \circ curve are the a posteriori error estimates from the regularized Stokes equations on uniform grids; the bottom \times curve are the a posteriori error estimates from the regularized Stokes equations on stretched grids. We observe that, for the $Q_2 - P_1$ method, a $2^6 \times 2^6$ stretched mesh grid can achieve a similar level of a posteriori error estimate as a $2^8 \times 2^8$ uniform mesh grid. Moreover, on the same level of mesh grid, i.e. $2^8 \times 2^8$, the a posteriori error estimate is significantly reduced from 6×10^{-2} to 6×10^{-3} .

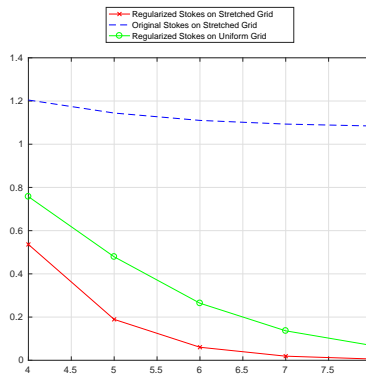


FIGURE 15. Plot of a Posteriori Error Estimates with $Q_2 - P_1$.

Acknowledgments

This research was partially supported by the National Science Foundation under the grants NSF-DMS1206438 and NSF-DMS1510249, and by the Research Fund of Indiana University.

References

- [1] Amann, Herbert, Navier-Stokes equations with nonhomogeneous Dirichlet data, *J. Nonlinear Math. Phys.*, 10, 2003, suppl. 1, 1–11.
- [2] Amann, Herbert, Nonhomogeneous Navier-Stokes equations with integrable low-regularity data, *Nonlinear problems in mathematical physics and related topics, II*, Int. Math. Ser. (N. Y.), 2, 1–28, Kluwer/Plenum, New York, 2002.
- [3] Amrouche, Chérif and Girault, Vivette, Decomposition of vector spaces and application to the Stokes problem in arbitrary dimension, *Czechoslovak Math. J.*, Czechoslovak Mathematical Journal, 44 (119), 1994, no. 1, 109–140.
- [4] C. Bardos, F. Di Plinio, and R. Temam, The Euler equations in planar nonsmooth convex domains, *J. Math. Anal. and Applications*, 407, 2013, 69–89.
- [5] J.D. Bozeman and C. Dalton, Numerical Study of viscous flow in a cavity, *Journal of Computational Physics*, Vol. 12, 1973, 348–363.
- [6] Olivier Botella, Numerical solution of Navier-Stokes singular problem by a Chebyshev projection method, Thesis, Université de Nice, France, 2012.
- [7] O.R. Burgaff, Analytical and Numerical studies of the structures of steady separated flows, *JFM*, Vol. 24, 1966, 113–151.
- [8] Lamberto Cattabriga, Su un problema al contorno relativo al sistema di equazioni di Stokes, *Rendiconti del Seminario Matematico della Università di Padova*. The Mathematical Journal of the University of Padova, 31, 1961, 308–340.
- [9] Q. Chen, Z. Qin and R. Temam, Numerical resolution near $t = 0$ of nonlinear evolution equations in the presence of corner singularities in space dimension 1, *Communications in Computational Physics*, CiCP, 9, No. 3, 2011, 568–586.
- [10] Q. Chen, Z. Qin and R. Temam, Treatment of incompatible initial and boundary data for parabolic equations in higher dimension, *Mathematics of Computation*, 80, 276, 2011, 2071–2096.
- [11] C. Cuvelier, A. Segal and A.A. van Steenhoven, Finite element methods and Navier-Stokes equations, *Mathematics and its Applications*, 22, D. Reidel Publishing Co., Dordrecht, 1986, xvi+483.
- [12] T. Davis, Direct methods for sparse linear systems, *Fundamental of Algorithms*, 2, Society for Industrial and Applied Mathematics (SIAM), Philadelphia, PA, 2006, xii+217.
- [13] J. Deny and J.L. Lions, Les espaces du type de Beppo Levi, *Université de Grenoble. Annales de l'Institut Fourier*, 5, 1953–54, 305–370.
- [14] F. Di Plinio and R. Temam, Grisvard's shift theorem near L^∞ and Yudovitch theory in polygonal domains, *SIAM J. of Nonlinear Analysis*, 47, No. 1, 2015, 159–178. DOI: 10.1137/130942632
- [15] D.A. Dunavant, High degree efficient symmetrical Gaussian quadrature rules for the triangle, *International Journal for Numerical Methods in Engineering*, 21, 6, 1985, 1129–1148.
- [16] E. Erturk, T.C. Corke, and C. Gokcol, Numerical Solutions of 2-D Steady Incompressible Driven Cavity Flow at High Reynolds Numbers, *International Journal for Numerical Methods in Fluids*, Vol. 48, 2005, 747–774.
- [17] H. Elman, D. Silvester and A. Wathen, Finite elements and fast iterative solvers, with application in incompressible fluid dynamics, Oxford University Press, Oxford, 2005.
- [18] Fabes, E. B. and Kenig, C. E. and Verchota, G. C., The Dirichlet problem for the Stokes system on Lipschitz domains, *Duke Math. J.*, 57, 1988, 3, 769–793.
- [19] Farwig, Reinhard and Galdi, Giovanni P. and Sohr, Hermann, Very weak solutions of stationary and instationary Navier-Stokes equations with nonhomogeneous data, *Nonlinear elliptic and parabolic problems*, Progr. Nonlinear Differential Equations Appl., 64, 113–136, Birkhäuser, Basel, 2005.
- [20] Farwig, Reinhard and Sohr, Hermann and Varnhorn, Werner and others, Local strong solutions of the nonhomogeneous Navier-Stokes system with control of the interval of existence, *Topological Methods in Nonlinear Analysis*, 46, 2, 999–1012 2015, Juliusz P. Schauder Centre for Nonlinear Studies.
- [21] Farwig, Reinhard and Galdi, Giovanni P. and Sohr, Hermann, A new class of weak solutions of the Navier-Stokes equations with nonhomogeneous data, *J. Math. Fluid Mech.*, 8, 2006, 3, 423–444.

- [22] Farwig, R. and Galdi, G. P. and Sohr, H., Very weak solutions and large uniqueness classes of stationary Navier-Stokes equations in bounded domains of \mathbb{R}^2 , *J. Differential Equations*, 227, 2006, 2, 564–580.
- [23] Farwig, Reinhard and Kozono, Hideo and Sohr, Hermann, Very weak, weak and strong solutions to the instationary Navier-Stokes system, *Topics on partial differential equations*, Jindřich Nečas Cent. Math. Model. Lect. Notes, 2, 1–54, Matfyzpress, Prague, 2007.
- [24] N. Flyer, Z. Qin and R. Temam, A penalty method for numerically handling dispersive equations with incompatible initial and boundary data, *Numerical Methods for Partial Differential Equations*, 28, 6, 2012, 1996–2009. DOI: 10.1002/num.21693
- [25] M. Fortin, R. Peyret, and R. Temam, Calcul des écoulements d'un fluide visqueux incompressible, *Proc. Second Intern. Conf. on Numerical Methods in Fluids Dynamics*, Lecture Notes in Physics, vol. 8, Springer-Verlag, 1971.
- [26] M. Fortin, R. Peyret and R. Temam, Résolution numérique des équations de Navier-Stokes pour un fluide incompressible, *J. Mécanique*, 10, 1971, 357–390.
- [27] Furioli, Giulia and Lemarié-Rieusset, Pierre G. and Terraneo, Elide, Unicité dans $L^3(\mathbb{R}^3)$ et d'autres espaces fonctionnels limites pour Navier-Stokes, *Rev. Mat. Iberoamericana*, 16, 2000, 3, 605–667.
- [28] Galdi, G. P. and Simader, C. G. and Sohr, H., A class of solutions to stationary Stokes and Navier-Stokes equations with boundary data in $W^{-1/q,q}$, *Math. Ann.*, 331, 2005, 1, 41–74,
- [29] Salvador Garcia, Aperiodic, chaotic lid-driven square cavity flows, *Math. Comput. Simulation*, 81 9, 2011, 1741–1769.
- [30] U. Ghia, K.N. Ghia, and C.T. Shin, High-Resolutions for incompressible flow using the Navier-Stokes equations and a multigrid method, *Journal of Computational Physics*, Vol. 48, 1982, 387–411.
- [31] J. M. Ghidaglia, Régularité des solutions de certains problèmes aux limites linéaires liés aux équations d'Euler, *Comm. Partial Differential Equations*, 9, (1984), no. 13, 1265–1298.
- [32] P. Grisvard, Singularities in boundary value problem, *Recherches en Mathématiques Appliquées*, Masson, Paris, Springer-Verlag, Berlin, 22, 1992, xiv+199
- [33] P. Grisvard, Elliptic problems in nonsmooth domains, *Monographs and Studies in Mathematics*, Pitman (Advanced Publishing Program), Boston, MA, 24, 1985, xiv+410.
- [34] J.-L. Guermond, C. Migeon, G. Pineau, and L. Quartapelle, Start-up flows in a three-dimensional rectangular driven cavity of aspect ratio 1:1:2 at $Re = 1000$, *Journal of Fluid Mechanics*, 450, 2002, 169–199.
- [35] Murlu M. Gupta, Ram P. Manohar, and Ben Noble, Nature of viscous flows near sharp corners, *Computers and Fluids*, 9, 4, 1981, 379–388.
- [36] Makram Hamouda and Abir Sboui, Boundary layers generated by singularities in the source function, *Asymptotic Analysis*, 93 (2015), no. 4, 281–310.
- [37] B. Héron, Quelques propriétés des applications de trace dans des espaces de champs de vecteurs à divergence nulle, *Communications in Partial Differential Equations*, 6, 12, 1981, 1301–1334. DOI: 10.1080/03605308108820212.
- [38] M.A. Kelmanson, Modified integral equation solution of viscous flows near sharp corners, *Computers & Fluids*, 11, 4, 1983, 307–324.
- [39] Kim, Hyunseok, Erratum to: Existence and regularity of very weak solutions of the stationary Navier-Stokes equations [MR2506072], *Arch. Ration. Mech. Anal.*, 196, 2010, 3, 1079–1080.
- [40] Kim, Hyunseok, Existence and regularity of very weak solutions of the stationary Navier-Stokes equations, *Arch. Ration. Mech. Anal.*, 193, 2009, 1, 117–152.
- [41] J.L. Lions, and E. Magenes, Non-homogeneous boundary value problems and applications, Vol. I, Springer-Verlag, New York-Heidelberg, 1972, xvi+357.
- [42] H.K. Moffatt, Viscous and resistive eddies near a sharp corner, *Journal of Fluid Mechanics*, 18, 1, 1963, 1–18.
- [43] Monniaux, Sylvie, Various boundary conditions for Navier-Stokes equations in bounded Lipschitz domains, *Discrete Contin. Dyn. Syst. Ser. S*, 6, 2013, 5, 1355–1369.
- [44] Nečas, Jindřich, Les méthodes directes en théorie des équations elliptiques, Masson et Cie, Éditeurs, Paris; Academia, Éditeurs, Prague, 1967, 351 pages.
- [45] Z. Qin and R. Temam, Penalty method for the KdV equations, *Applicable Analysis*, 91, No. 1-2, 2012, 193–211, DOI: 10.1080/00036811.2011.579564.

- [46] Raymond, Jean-Pierre, Feedback boundary stabilization of the two-dimensional Navier-Stokes equations, *SIAM J. Control Optim.*, 45, 2006, 3, 790–828 (electronic).
- [47] G. de Rham, Differentiable manifolds, *Grundlehren der Mathematischen Wissenschaften [Fundamental Principles of Mathematical Sciences]*, 266, Springer-Verlag, Berlin, 1984, x+167
- [48] W.W. Schultz, N.Y. Lee, N.Y. and J.P. Boyd, Chebyshev pseudospectral method of viscous flows with corner singularities, *Journal of Scientific Computing*, 4, 1, 1989, 1–23.
- [49] M.R. Schumak, and W.W. Schultz, Spectral method solution of the Stokes equations on nonstaggered grids, *Journal of Computational Physics*, 94, 1991, 30–58.
- [50] Denis Serre, Equations de Navier-Stokes stationnaires avec données peu régulières, *Annali della Scuola Normale Superiore di Pisa. Classe di Scienze. Serie IV*, 10, 4, 1983, 543–559.
- [51] Shen, Zhong Wei, A note on the Dirichlet problem for the Stokes system in Lipschitz domains, *Proc. Amer. Math. Soc.*, 123, 1995, 3, 801–811.
- [52] Shen, Zhong Wei, Boundary value problems for parabolic Lamé systems and a nonstationary linearized system of Navier-Stokes equations in Lipschitz cylinders, *Amer. J. Math.*, 113, 1991, 2, 293–373.
- [53] Serrin, James, On the interior regularity of weak solutions of the Navier-Stokes equations, *Arch. Rational Mech. Anal.*, 9, 1962, 187–195.
- [54] Jie Shen, Numerical simulation of the regularized driven cavity flows at high Reynolds numbers, *Spectral and high order methods for partial differential equations (Como, 1989)*, 273–280, North-Holland, Amsterdam, 1990
- [55] Sohr, Hermann, The Navier-Stokes equations, *Birkhäuser Advanced Texts: Basler Lehrbücher. [Birkhäuser Advanced Texts: Basel Textbooks]*, An elementary functional analytic approach, Birkhäuser Verlag, Basel, 2001, x+367 pages.
- [56] V.A. Solonnikov, Estimates for solutions of a non-stationary linearized system of Navier-Stokes equations, *Akademiya Nauk SSSR. Trudy Matematicheskogo Instituta imeni V.A. Stekova*, 70, 1964, 213–317.
- [57] V.A. Solonnikov, On the differential properties of the solution of the first boundary-value problem for a non-stationary system of Navier-Stokes equations, *Akademiya Nauk SSSR. Trudy Matematicheskogo Instituta imeni V.A. Stekova*, 73, 1964, 222–291.
- [58] Temam, Roger, Infinite-dimensional dynamical systems in mechanics and physics, *Applied Mathematical Sciences*, 68, Second Ed., Springer-Verlag, New York, 1997, xxii+648 pages.
- [59] Roger Temam, *Navier-Stokes Equations Theory and Numerical Analysis*, North-Holland Pub. Company, 1977. Reedition in the AMS-Chelsea Series, AMS-Providence, 2001.
- [60] Xiaoming Wang, A remark on the characterization of the gradient of a distribution, *Applicable Analysis*, 51, 1993, 35–40.
- [61] Le Zhang, Very weak solutions of the Stokes problem and its numerical simulations in a convex polygon, PhD, Indiana University, 2017.

¹ University of Tunis El Manar, Faculty of Sciences of Tunis, Department of Mathematics, Tunis, Tunisia.

E-mail, Makram Hamouda: mahamoud@indiana.edu

² The Institute for Scientific Computing and Applied Mathematics, Indiana University, 831 East Third Street, Bloomington, Indiana 47405, USA

E-mail, Roger Temam: temam@indiana.edu

E-mail, Le Zhang: zhangle@indiana.edu